Inorg. Chem. **2005**, *44*, 3657−3663

Iminic N-Bound Iminophosphorano versus Nitrilic N-Bound Iminophosphorano Os(IV) Complexes: A New Double Derivatization of the Nitrido Ligand

My Hang V. Huynh,*,† Thomas J. Meyer,*,‡ and Donald L. Jameson§

Dynamic Experimentation Division, DX-2: Materials Dynamics Group, MS C920, and The Associate Director for Strategic Research, MS A127, Los Alamos National Laboratory, Los Alamos, New Mexico 87545, and Department of Chemistry, Gettysburg College, Gettysburg, Pennsylvania 17325

Received February 5, 2005

The reactions between *trans*-[Os^{IV}(tpy)$(Cl)_2$(NCN)] (**1**) and PPh_3 and between *trans*-[Os^{IV}(tpy)$(Cl)_2(NPPh_3)]^+$ (**2**) and CN^- provide new examples of double derivatization of the nitrido ligand in an Os(VI)–nitrido complex ($Os^{VI}\equiv N$). The nitrilic N-bound product from the first reaction, *trans*-[Os^{II}(tpy)$(Cl)_2(NCNPPh_3)$] (**3**), is the coordination isomer of the first iminic N-bound product from the second reaction, *trans*-[Os^{II}(tpy)$(Cl)_2(N(CN)(PPh_3))$] (**4**). In CH_3CN at 45 °C, **4** undergoes isomerrization to **3** followed by solvolysis and release of (*N*-cyano)iminophosphorane, $NCNPPh_3$. These reactions demonstrate new double derivatization reactions of the nitrido ligand in $Os^{VI}\equiv N$ with its implied synthetic utility.

Introduction

Iminophosphoranes ($R_3P{=}NR$), which are electronically related to phosphorus ylides ($R_3P{=}CR_2$) and phosphine oxide ($R_3P{=}O$), have been extensively studied for their reactivity and for their usefulness as reagents for organic synthesis.[1] Their coordination chemistry is of interest because of the various η^1 and η^2 coordination modes that they display.[2] In particular, (*N*-cyano)iminophosphorane ($Ph_3P{=}N{-}C{\equiv}N$)[2a,3] and (α-cyano)phosphorus ylide ($Ph_3P{=}C(H){-}C{\equiv}N$)[4] have multiple bonding modes in transition metal complexes (Chart 1). These complexes have found numerous applications in organic synthesis[5] and as biological tools.[6]

There is no literature evidence for η^1-iminic N-bound iminophosphoranes in which N is datively bonded to the metal. In contrast, for η^1-ylidic C-bound phosphorus ylides, this is the most common coordination mode.

In earlier work, we demonstrated stepwise double addition to the nitrido ligand bound in *trans*-[Os^{VI}(tpy)$(Cl)_2$(N)]PF_6 (*trans*-[$Os^{VI}\equiv N]^+$) (2,2′:6′,2″-terpyridine) (eqs 1−3 in Scheme 1).[7a−e]

* Authors to whom correspondence should be addressed. E-mail: huynh@lanl.gov (M.H.V.H.); tjmeyer@lanl.gov (T.J.M.).

† Dynamic Experimentation Division, DX-2: Materials Dynamics Group, Los Alamos National Laboratory.

‡ The Associate Director for Strategic Research, MS A127, Los Alamos National Laboratory.

§ Department of Chemistry, Gettysburg College.

(1) (a) Arques, A.; Molina, P. *Curr. Org. Chem.* **2004**, *8*, 827−843. (b) Fresneda, P. M.; Molina, P. *Synlett* **2004**, *1*, 1−17. (c) Steiner, A.; Zacchini, S.; Richards, P. I. *Coord. Chem. Rev.* **2002**, *227*, 193−216 and references therein. (d) Hoesl, C. E.; Nefzi, A.; Houghten, R. A. *J. Comb. Chem.* **2003**, *5*, 155−160. (e) Johnson, A. W.; Kaska, W. C.; Starzewski, K. A. O.; Dixon, D. A. *Ylides and Imines of Phosphorus*; Wiley: New York, 1993; Chapter 13 and references therein. (f) Takahashi, M.; Suga, D. *Synthesis* **1998**, 986−990.

(2) (a) Falvello, L. R.; Fernandez, S.; Garcia, M. M.; Navarro, R.; Urriolabeitia, E. P. (*N*-cyano)iminophosphorane. *J. Chem. Soc., Dalton Trans.* **1998**, *22*, 3745−3750. (b) Kubo, K.; Nakazawa, H.; Inagaki, H.; Miyoshi, K. *Organometallics* **2002**, *21*, 1942−1948. (c) Carbo, M.; Falvello, L. R.; Navarro, R.; Soler, T.; Urriolabeitia, E. P. *Eur. J. Inorg. Chem.* **2004**, *11*, 2338−2347. (d) Fernandez, E. J.; Lopez-de-Luzuriaga, J. M.; Monge, M.; Olmos, E.; Laguna, A.; Villacampa, M. D.; Jones, P. G. *J. Cluster Sci.* **2000**, *11*, 153−167. (e) Fernandez, S.; Garcia, M. M.; Navarro, R.; Urriolabeitia, E. P. *J. Organomet. Chem.* **1998**, *561*, 67−76. (f) Streubel, R.; Wilkens, H.; Ostrowski, A.; Neumann, C.; Ruthe, F.; Jones, P. G. *Angew. Chem., Int. Ed.* **1997**, *36*, 1492−1494. (g) Falvello, L. R.; Fernandez, S.; Navarro, R.; Urriolabeitia, E. P. *Inorg. Chem.* **1997**, *36*, 1136−1142. (h) Belluco, U.; Michelin, R. A.; Bertani, R.; Facchin, G.; Pace, G.; Zanotto, L.; Mozzon, M.; Furlan, M.; Zangrando, E. *Inorg. Chim. Acta* **1996**, *252*, 355−366.

(3) (a) Bittner, S.; Pomerantz, M.; Assaf, Y.; Krief, P.; Xi, S. K.; Witczak, M. K. *J. Org. Chem.* **1988**, *53*, 1−5. (b) Veneziani, G.; Dyer, P.; Reau, R.; Bertrand, G. *Inorg. Chem.* **1994**, *33*, 5639−5642.

(4) (a) Falvello, L. R.; Fernandez, S.; Navarro, R.; Urriolabeitia, E. P. *Inorg. Chem.* **1997**, *36*, 1136−1142. (b) Nishiyama, H.; Itoh, K.; Ishii, Y. *J. Organomet. Chem.* **1975**, *87*, 129−135. (c) Weleski, E. T.; Silver, J. L.; Jansson, M. D.; Burmeister, J. L. *J. Organomet. Chem.* **1975**, *102*, 365−385.

10.1021/ic050203u CCC: $30.25
Published on Web 04/22/2005

Chart 1. Possible Coordination Modes of Iminophosphorane and Phosphorus Ylide

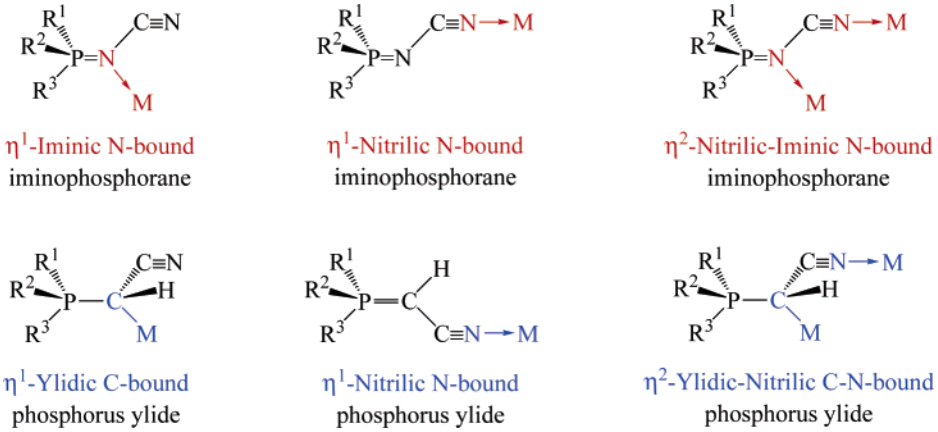

Scheme 1

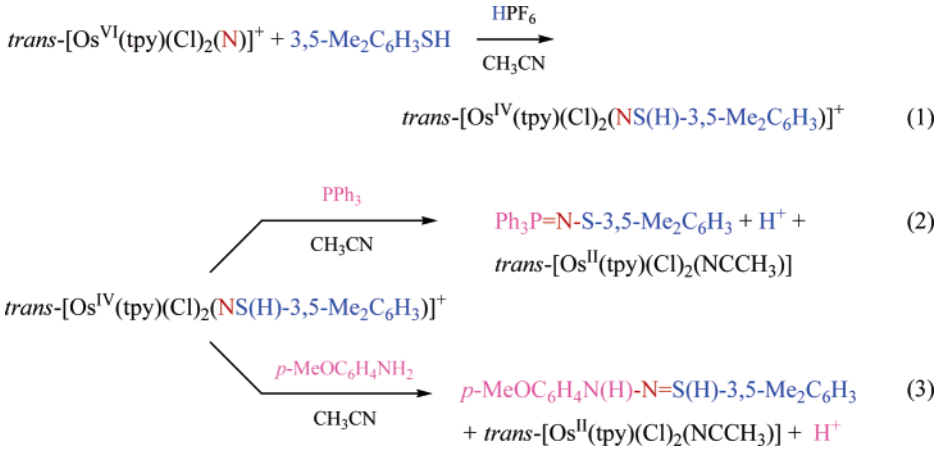

The combination of reactions in eq 1 followed by 2 or eq 1 followed by 3 demonstrates that *trans*-$[Os^{VI}{\equiv}N]^+$ is capable of undergoing successive two-electron, atom and group transfer reactions.[7a,b] In the examples shown, the sequential reactions involve formal N^- transfer followed by formal NS-3,5-$C_6H_3Me_2$ group transfer either to PPh_3 or to *p*-$MeOC_6H_4NH_2$. This reactivity opens new synthetic routes to doubly derivatized N compounds. It also demonstrates the transfer of large organic fragments by reactions analogous to O-atom and N^- transfers.

We recently reported an additional stepwise double addition to the nitrido ligand in *trans*-$[Os^{VI}{\equiv}N]^+$, as shown in eqs 4 and 5.[7e]

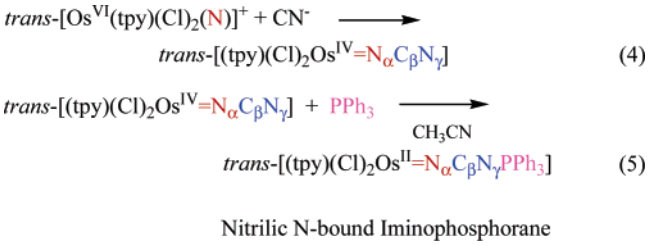

Nitrilic N-bound Iminophosphorane

When the reaction in eq 5 is carried out in the reverse order as shown in eq 6, the product is a second coordination isomer, *trans*-$[Os^{II}(tpy)(Cl)_2(N(CN)PPh_3)]$, which is the first example of an iminic N-bound iminophosphorano transition metal complex.

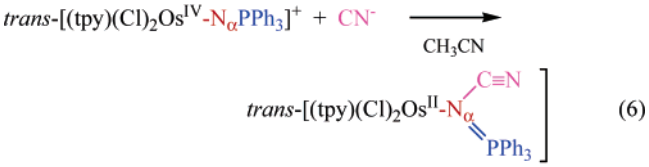

Iminic N-bound Iminophosphorane

Experimental Section

The following complexes and salts appear in this study: *trans*-$[Os^{VI}(tpy)(Cl)_2(N)]PF_6$ (*trans*-$[Os^{VI}{\equiv}N]PF_6$), *trans*-$[Os^{IV}(tpy)(Cl)_2$-

(5) (a) Lebel, H.; Paquet, V. *J. Am. Chem. Soc.* **2004**, *126*, 320−328. (b) Bertrand, G.; Cazaux, J. B.; Baceiredo, A.; Guerret, O.; Palacios, F.; Aparicio, D.; De los Santos, J. M. *C. R. Acad. Sci., Ser. IIc*: *Chim.* **2000**, *3*, 261−265. (c) Yasui, K.; Tamura, Y.; Nakatani, T.; Kawada, K.; Ohtani, M. *J. Org. Chem.* **1995**, *60*, 7567−7574. (d) Burland, M. C.; Meyer, T. Y. *Inorg. Chem.* **2003**, *42*, 3438−3444. (e) Hemming, K.; Bevan, M. J.; Loukou, C.; Patel, S. D.; Renaudeau, D. *Synlett* **2000**, *11*, 1565−1568.

(6) (a) Ding, M. W.; Yang, S. J.; Chen, Y. F. *Chin. J. Org. Chem.* **2004**, *24*, 923−926. (b) Tremblay, M. R.; Poirier, D. *Tetrahedron Lett.* **1999**, *40*, 1277−1280. (c) Bunuel, E.; Bull, S. D.; Davies, S. G.; Garner, A. C.; Savory, E. D.; Smith, A. D.; Vickers, R. J.; Watkin, D. *J. Org. Biomol. Chem.* **2003**, *1*, 2531−2542. (d) O'Dowd, H.; Ploypradith, P.; Xie, S. J.; Shapiro, T. A.; Posner, G. H. *Tetrahedron* **1999**, *55*, 3625−3636. (e) Shuto, S.; Niizuma, S.; Matsuda, A. *J. Org. Chem.* **1998**, *63*, 4489−4493.

(7) (a) Meyer, T. J.; Huynh, M. H. V. *Inorg. Chem.* **2002**, *42*, 8140−8160. (b) Huynh, M. H. V.; Jameson, D. L.; Meyer, T. J. *Inorg. Chem.* **2001**, *40*, 5062−5063. (c) Huynh, M. H. V.; White, P. S.; Carter, C. A. G.; Meyer, T. J. *Angew. Chem., Int. Ed.* **2001**, *40* (16), 3037−3039. (d) Huynh, M. H. V.; Baker, R. T.; Jameson, D. L.; Labouriau, A.; Meyer, T. J. *J. Am. Chem. Soc.* **2002**, *124*, 4580−4582. (e) Huynh, M. H. V.; Meyer, T. J.; Baker, R. T. *J. Am. Chem. Soc.* **2003**, *125*, 2832−2833.

(NCN)] (*trans*-[Os^{IV}═NCN]), *trans*-[Os^{II}(tpy)$(Cl)_2$(NCNPPh_3)] (*trans*-[Os^{II}−N≡C−N═PPh_3]), and *trans*-[Os^{II}(tpy)$(Cl)_2$(N(PPh_3)CN)] (*trans*-[Os^{II}−N(−C≡N)(═PPh_3)]).

Abbreviations and formulas used in the text include the following: TBAH = Bu_4NPF_6, tetrabutylammonium hexafluorophosphate; tpy = 2,2′:6′,2″-terpyridine; and bpy = 2,2′-bipyridine. The ligands are illustrated below:

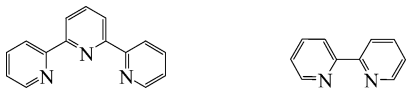

tpy bpy

Materials. House water was purified with a Barnstead E-Pure deionization system. High-purity acetonitrile was used as received from Aldrich. Osmium tetraoxide (>99%) was purchased from the Pressure Chemical Company. Triphenyl phosphine (PPh_3) and tetraethylammonium cyanide (Et_4NCN) were purchased from Aldrich and used without further purification. Deuterated solvents were purchased from Cambridge Isotope Laboratories and used as received. TBAH was recrystallized three times from boiling ethanol and dried under vacuum at 120° for 2 days. Other chemicals employed in the preparation of compounds were reagent grade and used without further purification.

Instrumentation and Measurement. Electronic absorption spectra were acquired by using a Hewlett-Packard model 8453 diode array UV−visible spectrophotometer in quartz cuvettes. Spectra in the near-IR region were recorded on a Perkin-Elmer Lambda 19 spectrophotometer by using a matched pair of 10 mm path length quartz cell. Elemental analyses were performed at Los Alamos National Laboratory and by Atlantic Microlabs (Norcross, GA). FT-IR spectra were recorded on a Nexus 670 FT-IR spectrophotometer at 4 cm^{-1} resolution interfaced with an IBM-compatible PC. IR measurements were made in Nujol Mulls. ^1H NMR spectra were obtained in DMSO-d_6 recorded on a JEOL-300 Fourier transform spectrometer. Organic products were analyzed by use of a Hewlett-Packard 5890 series II gas chromatograph with a 12 m × 0.2 mm × 0.33 μm HP-1 column (cross-linked methyl silicone gum) and a Hewlett-Packard 5971A mass selective detector, both interfaced with an HP Vectra PC computer system.

Kinetic studies by UV−visible monitoring were conducted on a Hewlett-Packard 8453 diode array spectrophotometer interfaced with an IBM-compatible PC. The measurements were made in standard quartz 1 cm path length cuvettes. All kinetic studies were performed at 25.0 ± 0.1 °C with a pseudo-first-order excess of organic reagents. Kinetic studies of *trans*-[Os^{IV}-NCN] with PPh_3 and of *trans*-[Os^{IV}−NPPh_3]$^+$ with Et_4NCN were performed in DMF. The concentrations of the Os(IV) solutions were 7.5×10^{-4} M for *trans*-[Os^{IV}═NCN] and 8.0×10^{-4} M for *trans*-[Os^{IV}−NPPh_3]$^+$. The concentrations of PPh_3 or Et_4NCN were varied from 8.15×10^{-3} M to 9.15×10^{-2} M for PPh_3 and from 5.5×10^{-4} M to 5.5×10^{-3} M for Et_4NCN. The temperature of solutions during the kinetic studies was maintained to within ±0.1 °C with use of a RTE-7 Thermo-Neslab circulating water bath.

Cyclic voltammetric experiments were measured with the use of PAR model 263 and 273 potentiostats. Bulk electrolyses were performed with a PAR model 173 potentiostat/galvanostat. Cyclic voltammetry measurements were conducted in a three-compartment cell with 0.2 M TBAH as the supporting electrolyte and a 1.0 mm platinum-working electrode for CH_3CN or DMF. All potentials are referenced to the saturated sodium chloride calomel electrode (SSCE, 0.236 V vs NHE) at room temperature and are uncorrected for junction potentials. In all cases, the auxiliary electrode was a platinum wire. The solution in the working compartment was deoxygenated by N_2 bubbling.

Synthesis and Characterization. The following complexes and compounds were prepared by literature procedures: *trans*-[Os^{VI}(tpy)$(Cl)_2$(N)]PF_6,[8a] *mer*-[Os^{VI}(bpy)$(Cl)_3$(N)],[8b] *trans*-[Os^{IV}(tpy)$(Cl)_2$(NCN)],[7c] *mer*-Et_4N[Os^{IV}(bpy)$(Cl)_3$(NCN)],[7c] and *trans*-[Os^{IV}(tpy)$(Cl)_2$(NPPh_3)]PF_6.[9]

***trans*-[Os^{IV}(tpy)$(Cl)_2$(NCN)].** In a 100 mL round-bottom flask, *trans*-[Os^{VI}≡N]$^+$ (200 mg, 0.306 mmol) was stirred in 50 mL of CH_2Cl_2 under N_2 atmosphere for 2 min. One equivalent of NEt_4CN (47.8 mg) in 5 mL of CH_2Cl_2 was bubbled with N_2 for 2 min and added to the solution of *trans*-[Os^{VI}≡N]$^+$. The reaction mixture was stirred continuously under N_2 for 30 min. The brown precipitate was filtered, washed thoroughly with fresh CH_2Cl_2, and air-dried. Yield: 148 mg (91%). Anal. Calcd for $OsC_{16}H_{11}N_5Cl_2$: C, 35.96; H, 2.07; N, 13.11. Found: C, 36.17; H, 2.15; N, 13.32. UV−visible data (DMF) λ_{max}, nm (ϵ, M^{-1} cm^{-1}): 867 (3.28×10^2), 744 (7.83×10^2), 628 (2.87×10^3), 512 (6.03×10^3), 416 (8.40×10^3), 318 (3.26×10^4), and 280 (2.95×10^4). Cyclic voltammetric data in 0.1 M TBAH/DMF (V vs SSCE): $E_{1/2}$(Os(VI/V)) = +1.72 V, $E_{1/2}$(Os(V/IV)) = +0.90 V, $E_{1/2}$(Os(IV/III)) = −0.40 V, and $E_{1/2}$(Os(III/II)) = −1.30 V. Infrared (cm^{-1}, Nujol): ν(C≡N_β) = 1938 cm^{-1}; ν(tpy) 1466 (vs), 1456 (vs), and 1369 (vs).

***trans*-[Os^{II}(tpy)$(Cl)_2$(NCNPPh_3)].** In a 100 mL Erlenmeyer flask, *trans*-[Os^{IV}═NCN] (300 mg, 0.561 mmol) was stirred in 30 mL of CH_3CN under N_2. One equivalent of PPh_3 (147 mg) in 5 mL of CH_3CN was added, and the reaction mixture was stirred for 1 h. The brown solution was evaporated to 5 mL by rotary evaporation. Upon addition of 150 mL of Et_2O, the brown product was filtered, washed with fresh Et_2O, and air-dried. Yield: 0.423 g (95%). Anal. Calcd for $OsC_{34}H_{26}N_5Cl_2P$: C, 51.26; H, 3.29; N, 8.79. Found: C, 51.40; H, 3.48; N, 8.97. Cyclic voltammetric data in 0.1 M Bu_4NPF_6/DMF (V vs SSCE): $E_{1/2}$(Os(IV/III)) = +1.12 V and $E_{1/2}$(Os(III/II)) = −0.16 V. Infrared (cm^{-1}, Nujol) for **Os^{II}−^{14}NCNPPh_3:** ν($^{14}N_\alpha$≡C) = 2235 cm^{-1}; ν(tpy) 1467 (vs), 1447 (vs), and 1440 (vs); ν($^{14}N_\beta$═P) = 1116 cm^{-1}. Infrared for **Os^{II}−^{15}NCNPPh_3:** ν($^{15}N_\alpha$≡C) = 2205 cm^{-1}; ν(tpy) 1465 (vs), 1446 (vs), and 1441 (vs); ν($^{14}N_\beta$═P) = 1116 cm^{-1}. ^1H NMR (δ, DMSO-D_6): 11 H for tpy: (2 H, d) 8.32 → 8.29; (2 H, d) 8.07 → 8.04, (2 H, d) 7.99 → 7.96; (2 H, t) 7.37 → 7.33; (2 H, t) 7.23 → 7.17; (H, t) 6.29 → 6.25; 15 H for PPh_3: 7.88 → 7.69. ^{31}P NMR (δ, DMSO-D_6): 26.5 ppm. UV−visible spectra in DMF (λ_{max}, nm (ϵ, M^{-1} cm^{-1}): 750 (2.58×10^3), 660 (3.47×10^3), 592 (5.64×10^3), 502 (7.03×10^3), 424 (7.95×10^3), 386 (9.56×10^3), and 330 (2.14×10^4).

***trans*-[Os^{II}(tpy)$(Cl)_2$(N(CN)PPh_3)].** In a 100 mL Erlenmeyer flask, *trans*-[Os^{IV}-NPPh_3]$^+$ (400 mg, 0.519 mmol) was stirred in 40 mL of CH_3CN under N_2. One equivalent of Et_4NCN (81.1 mg) in 5 mL of CH_3CN was added, and the reaction mixture was stirred for 30 min. The solvent was removed by rotary evaporation. The product was filtered, washed with Et_2O, and air-dried. Yield: 0.389 g (94%). Anal. Calcd for $OsC_{34}H_{26}N_5Cl_2P$: C, 51.26; H, 3.29; N, 8.79. Found: C, 51.57; H, 3.38; N, 8.89. Cyclic voltammetric data

(8) (a) Pipes, D. W.; Bakir, M.; Vitols, S. E.; Hodgson, D. J.; Meyer, T. J. *J. Am. Chem. Soc.* **1990**, *112*, 5507−5514. (b) Demadis, K. D.; El-Samanody, El.-S.; Meyer, T. J.; White, P. S. *Inorg. Chem.* **1998**, *37*, 838−839. (c) Ware, D. C.; Taube, H. *Inorg. Chem.* **1991**, *30* (24), 4605−4610.

(9) (a) Bakir, M.; White, P. S.; Dovletoglou, A.; Meyer, T. J. *Inorg. Chem.* **1991**, *30*, 2835−2836. (b) Demadis, K. D.; Bakir, M.; Klesczewski, B. G.; Williams, D. S.; White, P. S.; Meyer, T. J. *Inorg. Chim. Acta* **1998**, *270*, 511−526.

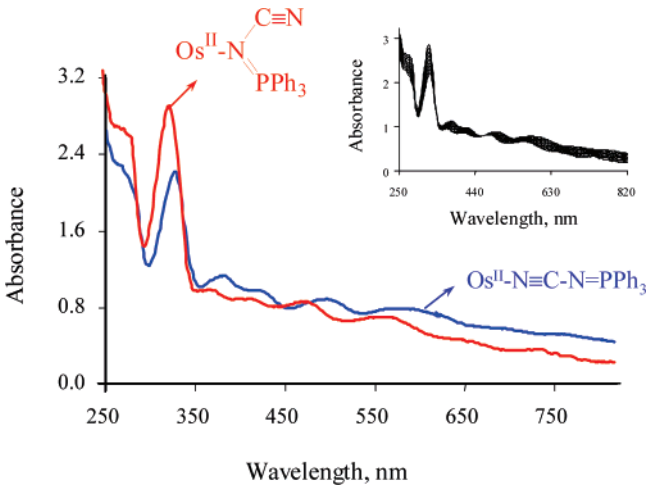

Figure 1. Effect of the order of addition on electronic absorption spectra for nitrilic N-bound and iminic N-bound Os(II) complexes

in 0.1 M Bu_4NPF_6/DMF (V vs SSCE): $E_{1/2}$(Os(IV/III)) = +1.25 V and $E_{1/2}$(Os(III/II)) = −0.07 V. Infrared (cm^{-1}, Nujol) for **Os^{II}−^{14}N(CN)PPh_3:** ν(C≡N) = 2152 cm^{-1}; ν(tpy) 1485 (vs), 1468 (vs), and 1453 (vs); $\nu(^{14}N_\beta{=}P)$ = 1103 cm^{-1}. Infrared for **Os^{II}−^{15}N(CN)PPh_3:** ν(C≡N) = 2152 cm^{-1}; ν(tpy) 1483 (vs), 1466 (vs), and 1441 (vs); $\nu(^{15}N_\beta{=}P)$ = 1087 cm^{-1}. ^{31}P NMR (δ, DMSO-D_6): 16.6 ppm. UV−visible spectra in DMF (λ_{max}, nm (ϵ, M^{-1} cm^{-1}): 738 (1.71 × 10^3), 650 (2.58 × 10^3), 564 (4.78 × 10^3), 476 (6.84 × 10^3), 416 (7.00 × 10^3), 372 (8.15 × 10^3), and 326 (2.81 × 10^4).

Results

Reaction between *trans*-[Os^{IV}(tpy)$(Cl)_2(N_\alpha C_\beta N_\gamma)$] (*trans*-[$Os^{IV}$−$N_\alpha C_\beta N_\gamma$]) and PPh_3. In an earlier report, we described an oxo-like reactivity for the Os(IV)−cyanoimido complexes, *trans*-[Os^{IV}(tpy)$(Cl)_2(N_\alpha C_\beta N_\gamma)$] and *mer*-[$Os^{IV}(bpy)(Cl)_3(N_\alpha C_\beta N_\gamma)]^-$.[7c] This analogy extends to the reaction of the former with PPh_3 to give an Os(II) nitrilic N-bound iminophosphorano product (eqs 4 and 5).[7e]

The *trans*-[Os^{II}−NCNPPh_3] product was isolated in 95% yield and characterized by elemental analysis, cyclic voltammetry, infrared, ^{1}H and ^{31}P NMR, and UV−visible spectroscopies. As found earlier in reactions with olefins,[7e] reaction with PPh_3 occurs at the remote N_γ site of the cyanoimido ligand. The site of attack is revealed in the ^{15}N labeling experiment, *trans*-[$Os^{IV}{=}^{15}N{-}C{\equiv}^{14}N$] + PPh_3 → *trans*-[$Os^{II}{-}^{15}N{\equiv}C{-}^{14}N{=}PPh_3$] by IR measurements. For the ^{15}N-labeled product, there is a shift of 30 cm^{-1} in ν(N≡C) and no shift in ν(N=P) consistent with the isotopic distribution *trans*-[$Os^{II}{-}^{15}N{\equiv}C{-}^{14}N{=}PPh_3$] rather than *trans*-[$Os^{II}{-}^{14}N{\equiv}C{-}^{15}N{=}PPh_3$].

The kinetics of the reaction in eq 5 were studied by conventional mixing with UV−visible monitoring and PPh_3 present in pseudo-first-order excess. The spectrum of *trans*-[Os^{II}−N≡C−N=PPh_3] is shown in Figure 1. The rate law resulting from the kinetics study is given in eq 7 with $k_{obs} = k[PPh_3]$ and k = (6.5 ± 0.1) × 10^{-2} s^{-1}. Once formed, *trans*-[Os^{II}−N≡C−N=PPh_3] undergoes solvolysis with the reaction complete after refluxing under N_2 for 24 h (eq 8).

$$\frac{-\,d[Os^{VI}{\equiv}N^+]}{dt} = k\,[Os^{IV}{=}N{-}C{\equiv}N]\,[PPh_3] = k_{obs}\,[Os^{IV}{=}N{-}C{\equiv}N] \quad (7)$$

$$trans\text{-}[(tpy)(Cl)_2Os^{II}\text{-}N{\equiv}C\text{-}N{=}PPh_3] \xrightarrow{CH_3CN} trans\text{-}[(tpy)(Cl)_2Os^{II}\text{-}N{\equiv}CCH_3] + N{\equiv}C\text{-}N{=}PPh_3 \quad (8)$$

The organic product was extracted with *n*-hexane and characterized by GC−MS (m/z = 302) and ^{31}P NMR (δ = 25.71 ppm). This reaction reinforces the earlier observation that Os(IV) adducts are capable of undergoing a second group transfer reaction to give a doubly derivatized N-compound. In the transfer in eq 8, the reaction formally involves transfer of NCN^0 analogous to oxo transfer. The subsequent solvolysis and release of the (*N*-cyano)iminophosphorane product, $NCNPPh_3$, demonstrate that the reaction has potential synthetic utility.

Reaction between *trans*-[Os^{IV}(tpy)$(Cl)_2$(NPPh_3)]$^+$ (*trans*-[Os^{IV}−NPPh_3]$^+$) and CN^-. It was possible to study the same reaction sequence but in reverse order because of the availability of *trans*-[Os^{IV}(tpy)$(Cl)_2$(NPPh_3)]$^+$ from a previous study.[9] The reaction between *trans*-[$Os^{IV}{-}N_\alpha PPh_3]^+$ and Et_4NCN occurs by attack of CN^- at N_α to give the iminic N-bound iminophosphorano product, *trans*-[(tpy)$(Cl)_2Os^{II}{-}N_\alpha$(CN)PPh_3] (eq 6).

This product was isolated in 94% yield and characterized by elemental analysis, cyclic voltammetry, UV−visible, infrared including ^{15}N labeling, and ^{1}H NMR spectroscopies. It is a coordination isomer of the product of the reaction in eq 6 as evidenced by ^{15}N labeling and IR measurements, the common elemental compositions, the differences in UV−visible spectra (Figure 1), and $E_{1/2}$ values for the Os(IV/III) and Os(III/II) couples. Attack at N_α was shown by IR.

The sequential addition reactions demonstrate the use of a metal center as a template for the synthesis of novel organic compounds. The overall procedure begins with the synthesis of $Os^{VI}{\equiv}N$, followed by sequential addition of the nucleophiles (Nu_1) to form $Os^{IV}{=}NNu_1$ followed by the second (Nu_2) to give $Os^{II}{=}N(Nu_1)(Nu_2)$. Given the expense of Os, the synthetic utility of the method is limited, but in principle, the double addition protocol may find use based on other metal complexes with similar properties. The organic target in this case was N≡C−N=PPh_3, but the procedure is quite general and may provide a general route to heteroatom compounds of the form $(Nu_2)N(Nu_1)$ or $(Nu_2)N(H)(Nu_1)$.

Comparison and Characterizations. Examples of Pt complexes containing the nitrilic N-bound ligand N≡C−N=PPh_3,[2a] [Pt(C−P)(PPh_3)(N≡C−N=PPh_3)]ClO_4 (C−P = *o*-$CH_2C_6H_4P$(*o*-$CH_3C_6H_4)_2$), have been reported from the reaction between [Pt(C−P)(PPh_3)(NCCH_3)]ClO_4 and the preformed N≡C−N=PPh_3 ligand.[3a] Through ligand substitution reaction pathways, the iminophosphorane N≡C−N=PPh_3 ligand selectively coordinates through the nitrilic N-bound rather than through iminic N-bound. There was no evidence for the formation of iminic N-bound N≡C−N=PPh_3. This poor coordinative ability may be due to the delocalization of the electron density resulting in a

Scheme 2

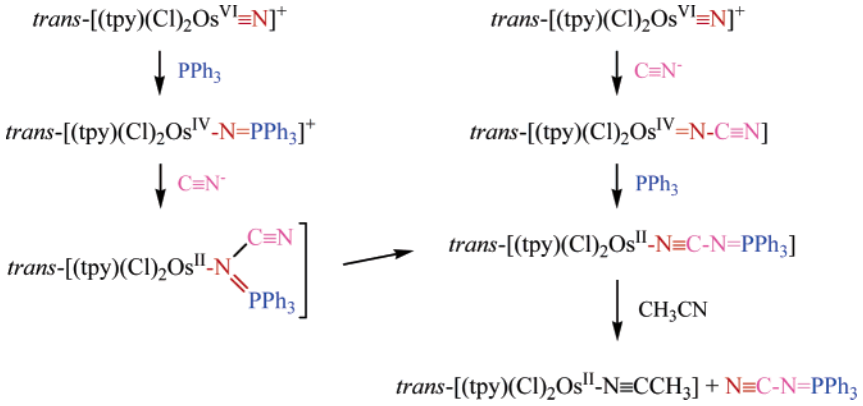

lower charge density at the iminic N-atom. For instance, both carbonylic O-atom and pyridinic N-atom of $Ph_3PNC(O)$-2-py[10] coordinate to transition metals even though their coordinative abilities are approximately the same as that of the iminic N-atom. By using the same reaction conditions with $[Pd(Cl)_2(NCPh)_2]$ as the precursor, $Ph_3P{=}C(H)CN$ selectively coordinated to Pd through the ylidic C-atom, while $N{\equiv}C{-}N{=}PPh_3$ primarily bonded to Pd via the nitrilic N-atom.[2a]

In the IR spectra of *trans*-$[Os^{II}{-}{}^{14}N{-}(C{\equiv}{}^{14}N){=}PPh_3]$ and *trans*-$[Os^{II}{-}{}^{15}N{-}(C{\equiv}{}^{14}N){=}PPh_3]$, $\nu(C{\equiv}{}^{14}N)$ appears for both complexes at 2152 cm^{-1}, while $\nu({}^{15}N{=}P)$ appears at 1087 cm^{-1} for the latter and $\nu({}^{14}N{=}P)$ at 1103 cm^{-1} for the former. A strong absorption at 2235 cm^{-1} attributed to the $N{\equiv}C{-}N{=}PPh_3$ stretch is higher in energy with respect to that at 2176 cm^{-1} in the free ligand, and both are higher than the band at 2152 cm^{-1} attributed to $N(C{\equiv}N){=}PPh_3$. The nitrilic N-bound absorption at 2235 cm^{-1} in *trans*-$[Os^{II}(tpy)(Cl)_2(NCNPPh_3)]$ is comparable to the band at 2256 cm^{-1} in *trans*-$[Pd(Cl)_2(NCNPPh_3)]$ and (to) 2215 and 2228 cm^{-1} in *trans*-$[Pd(C{-}P)(NCNPPh_3)_2]$.

The ^{31}P NMR resonance at 16.59 ppm for the iminic N-bound ligand is shifted upfield by 9 ppm, while the resonance at 26.49 ppm for the nitrilic N-bound ligand is shifted downfield by 0.8 ppm. The resonance for the nitrilic N-bound ligand in *trans*-$[Os^{II}{-}{}^{14}N{\equiv}C{-}N{=}PPh_3]$ is comparable to those of the nitrilic N-bound ligand for *trans*-$[Pd(C{-}P)(NCNPPh_3)]$ (27.76 and 29.18 ppm) and *trans*-$[Pt(C{-}P)(NCNPPh_3)_2]$ (28.06 and 29.52 ppm).

When the iminic N-bound iminophosphorano isomer is heated to 45 °C for 5 h in CH_3CN, isomerization occurs to give the nitrilic N-bound iminophosphorano complex (eq 9), as shown by the changes in UV−Visible spectra in Figure 1. Isomerization is followed by solvolysis (eq 8) as for the nitrilic N-bound iminophosphorano isomer.

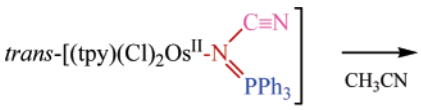

trans-$[(tpy)(Cl)_2Os^{II}{-}N{\equiv}C{-}N{=}PPh_3]$ (9)

(10) Falvello, L. R.; Garcia, M. M.; Lazaro, I.; Navarro, R.; Urriolabeitia, E. P. *New J. Chem.* **1999**, *23*, 227−235.

Discussion

Sequential Addition Reaction Pathways. The reactions between *trans*-$[Os^{IV}{-}NCN]$ and PPh_3 and between *trans*-$[Os^{IV}{-}NPPh_3]^+$ and CN^- provide additional examples of double derivatization of the nitrido group in *trans*-$[Os^{VI}{\equiv}N]^+$. These are stepwise reactions with N^- transfer followed by group transfer, $[NCN]^0$ in eq 5 and $[NPPh_3]^0$ in eq 6. The final products contain the nitrilic N-bound $N{\equiv}C{-}N{=}PPh_3$ and iminic N-bound $N{\equiv}C{-}N{=}PPh_3$ ligands. Both products are coordinatively stable at room temperature in CH_3CN but undergo solvolysis (eq 8) or isomerization (eq 9) followed by solvolysis. The ability to vary the order of addition in this case results in the preparation of the first iminic N-bound transition metal complex. A summary of the reactions involved is shown in Scheme 2.

As noted in the Introduction, double addition to a nitrido N-atom has also been observed in the sequence beginning with reaction between 3,5-$Me_2C_6H_3SH$ and *trans*-$[Os^{VI}{\equiv}N]^+$ followed by $[NSC_6H_3Me_2]^0$ transfer to PPh_3. These reaction sequences are notable because they show that (i) Os(VI)−nitrido complexes are capable of undergoing successive two-electron, atom (N^-) transfer followed by group transfer reactions; (ii) the reactivity can be applied in general way to the synthesis of organic heteroatom compounds; and (iii) the redox step for the second reaction with Os(IV) is conceptually the same as N^- transfer in eq 1 but with transfer of a large organic fragment (e.g., $[NS\text{-}3,5\text{-}Me_2C_6H_3]^0$ transfer in eq 2, $[NCN]^0$ transfer in eq 5, and $[NPPh_3]^0$ transfer in eq 6).

Factors Affecting Sequential Addition Reactions. The order in which the sequential reactions are carried out can be important. Unlike the reversible reaction sequences shown in eq 4 followed by eq 5 and eq 10 followed by eq 6, the reverse order of the sequence shown in eqs 1 and 2, which is eq 10 followed by eq 11, does not occur.

Trans-$[Os^{VI}(tpy)(Cl)_2(N)]^+ + PPh_3 \longrightarrow$ *trans*-$[Os^{IV}(tpy)(Cl)_2(NPPh_3)]^+$ (10)

Trans-$[Os^{IV}(tpy)(Cl)_2(NPPh_3)]^+ + Me_2C_6H_3SH \longrightarrow$ NR (11)

The origin of the effect is electronic and not steric. As

Chart 2

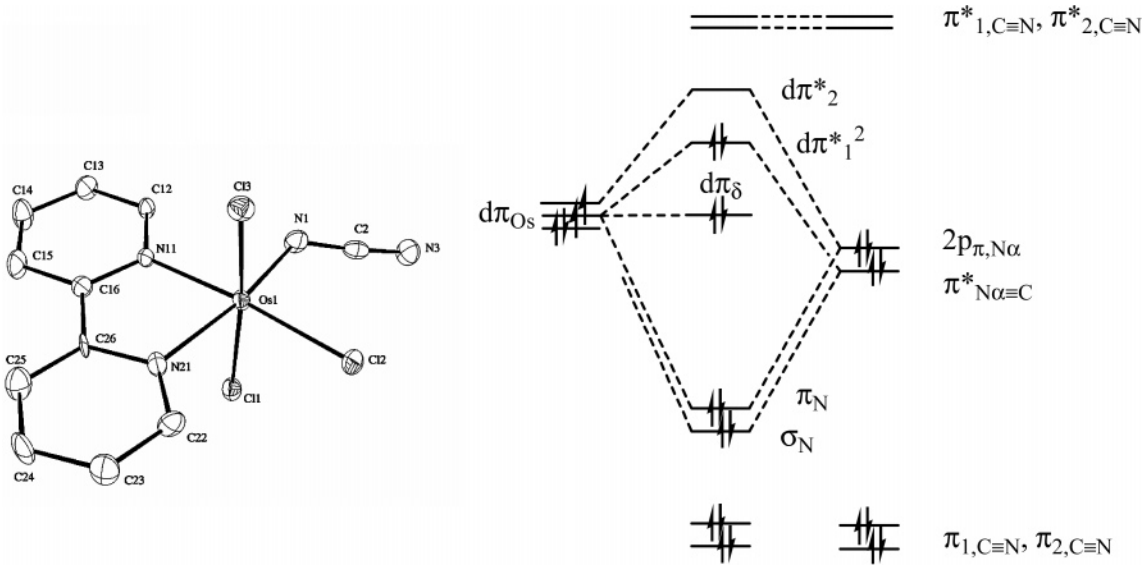

illustrated in eq 12, oxidation of *trans*-[Os^{IV}−NPPh$_3$]$^+$ to *trans*-[Os^{V}−NPPh$_3$]$^{2+}$ triggers the second reaction, which is followed by solvolysis, and gives the expected organic product.

$$\textit{Trans}\text{-}[Os^{IV}(tpy)(Cl)_2(NPPh_3)]^+ \xrightarrow{-\,e^-} \textit{trans}\text{-}[Os^{V}(tpy)(Cl)_2(NPPh_3)]^{2+} \quad (12)$$

$$\textit{Trans}\text{-}[Os^{V}(tpy)(Cl)_2(NPPh_3)]^{2+} + Me_2C_6H_3SH \longrightarrow \textit{trans}\text{-}[Os^{III}(tpy)(Cl)_2(NCCH_3)]^+ + Ph_3P{=}N\text{-}S\text{-}3,5\text{-}Me_2C_6H_3 + H^+ \quad (13)$$

Molecular Electronic Structure Correlations. A schematic energy ordering diagram for *mer*-[Os^{IV}−NCN]$^-$ and the structure of the complex[7c] are shown in Chart 2. The energy diagram is taken from a scheme used to describe the bonding in Os(IV)−hydrazido complexes, *trans*-[Os^{V}(tpy)(Cl)$_2$(NNR$_2$)]$^+$.[10] It features dπ−π mixing between dπ(Os) orbitals and both 2p$_{\pi,N\alpha}$ and a filled π*(N$_\alpha$≡C) orbital on the NCN^{2-} ligand.

Experimental evidence for this or a related orbital pattern comes from the diamagnetism of *trans*-[Os^{IV}−NCN] as shown by ^{1}H NMR and by the appearance of low energy absorption bands at 876 (1.15×10^4 cm^{-1}) and 744 nm (1.34×10^4 cm^{-1}). The latter can be assigned to the d$\pi \rightarrow$ dπ interconfigurational transitions $^1[(d\pi_\delta)^2(d\pi^*_1)^2] \rightarrow {}^1[(d\pi_\delta)^2(d\pi^*_1)^1(d\pi^*_2)^1]$ and $^1[(d\pi_\delta)^2(d\pi^*_1)^2] \rightarrow {}^1[(d\pi_\delta)^1(d\pi^*_1)^2(d\pi^*_2)^1]$, respectively. For the corresponding hydrazido[10] and N$_\beta$-methoxyhydrazido[11] complexes, these bands appear at 975 and 859 nm and at 883 and 666 nm, respectively. This shows that the same pattern of dπ orbitals exists in all three complexes. These are presumably singlet → singlet transitions with the corresponding singlet → triplet transitions present at lower energy and of diminished intensity.

Based on the band energies and assuming a constant pairing energy, the energy difference (ΔE) between dπ^*_2 and dπ^*_1 is 1.90×10^3 cm^{-1}. The dπ* splitting for *trans*-[Os^{IV}(tpy)(Cl)$_2$(N(H)N(CH$_2$)$_4$O)]$^+$ [9] is 1.30×10^3 cm^{-1}, and it is 3.70×10^3 cm^{-1} for *trans*-[Os^{IV}(tpy)(Cl)$_2$(N(H)N(H)(OMe))]$^+$.[11] This is consistent with the diamagnetism of the complex and with the dπ−π orbital ordering in Chart 2.

Adjacent-N$_\alpha$ versus Remote-N$_\gamma$ "Attack". In the reaction between *trans*-[Os^{IV}−N$_\alpha$C$_\beta$N$_\gamma$] and PPh$_3$, it is notable that the site of PPh$_3$ attack is at the remote nitrogen, N$_\gamma$, rather than at the adjacent nitrogen, N$_\alpha$. The reactions between *trans*-[Os^{IV}−NPPh$_3$]$^+$ and CN$^-$ in eq 6 and between *trans*-[Os^{IV}−NS(H)C$_6$H$_3$Me$_2$]$^+$ and PPh$_3$ in eq 2 show that N$_\alpha$ is an accessible site for redox addition. In Chart 2, dπ^*_2 is empty and accessible for an initial electron pair interaction. Furthermore, electron flow and a change in hybridization at N$_\alpha$ from sp to sp^2 create a bonding pathway for N$_\alpha$ redox addition as shown in eq 14 for CN$^-$ addition to *trans*-[Os^{IV}−NPPh$_3$]$^+$.

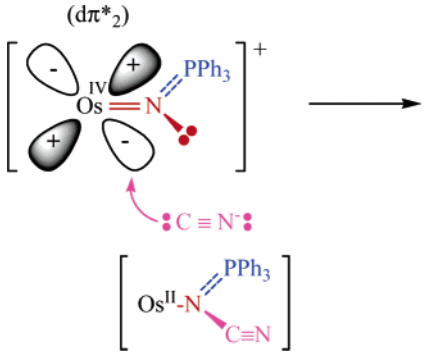

(14)

By contrast, addition of PPh$_3$ to *trans*-[Os^{IV}−NCN] occurs at the remote N$_\gamma$ site as shown by the ^{15}N labeling study. In this case, the LUMO for initial electron pair interaction is a $\pi^*_{C\equiv N}$ orbital. As shown below in equation 15, subsequent

(11) Huynh, M. H. V.; El-Samanody, E.-S.; Demadis, K. D.; White, P. S.; Meyer, T. J. *Inorg. Chem.* **2000**, *39*, 3075−3085.
(12) Huynh, M. H. V.; Meyer, T. J.; Hiskey, M. A.; Jameson, D. L. *J. Am. Chem. Soc.* **2004**, *126*, 3608−3615.

electron transfer to Os(IV) and a change in hybridization at N_γ from sp to sp^2 results in the final product (eq 15).

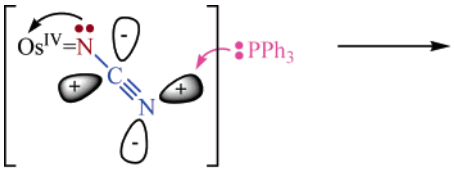

(π^*_{CN})

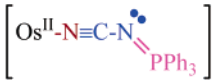

(15)

There is precedence for "remote" attach at N_γ in the reactions between *trans*-[Os^{IV}(tpy)$(Cl)_2$(NCN)] or *mer*-[Os^{V}(bpy)$(Cl)_3$(NCN)] and olefins as shown by ^{15}N labeling and infrared measurements (eq 16).[7e]

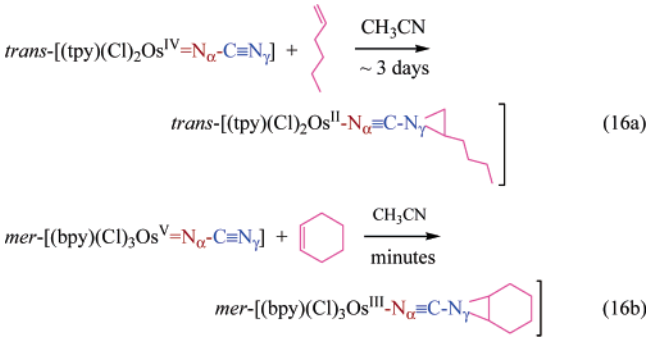

Acknowledgment. We acknowledge the Laboratory Directed Research and Development Program for support of this research. Los Alamos National Laboratory is operated by the University of California for the U.S. Department of Energy under Contract W-7405-ENG-36.

IC050203U